Enhanced Expression of the α7β1 Integrin Reduces Muscular Dystrophy and Restores Viability in Dystrophic Mice✪

Dean J. Burkin,* Gregory Q. Wallace,* Kimberly J. Nicol,* David J. Kaufman,‡ and Stephen J. Kaufman*

*Department of Cell and Structural Biology, University of Illinois, Urbana, Illinois 61801; and ‡National Cancer Institute, Bethesda, Maryland 20892

Abstract. Muscle fibers attach to laminin in the basal lamina using two distinct mechanisms: the dystrophin glycoprotein complex and the α7β1 integrin. Defects in these linkage systems result in Duchenne muscular dystrophy (DMD), α2 laminin congenital muscular dystrophy, sarcoglycan-related muscular dystrophy, and α7 integrin congenital muscular dystrophy. Therefore, the molecular continuity between the extracellular matrix and cell cytoskeleton is essential for the structural and functional integrity of skeletal muscle. To test whether the α7β1 integrin can compensate for the absence of dystrophin, we expressed the rat α7 chain in *mdx/utr*$^{-/-}$ mice that lack both dystrophin and utrophin. These mice develop a severe muscular dystrophy highly akin to that in DMD, and they also die prematurely. Using the muscle creatine kinase promoter, expression of the α7BX2 integrin chain was increased 2.0–2.3-fold in *mdx/utr*$^{-/-}$ mice. Concomitant with the increase in the α7 chain, its heterodimeric partner, β1D, was also increased in the transgenic animals. Transgenic expression of the α7BX2 chain in the *mdx/utr*$^{-/-}$ mice extended their longevity by threefold, reduced kyphosis and the development of muscle disease, and maintained mobility and the structure of the neuromuscular junction. Thus, bolstering α7β1 integrin–mediated association of muscle cells with the extracellular matrix alleviates many of the symptoms of disease observed in *mdx/utr*$^{-/-}$ mice and compensates for the absence of the dystrophin- and utrophin-mediated linkage systems. This suggests that enhanced expression of the α7β1 integrin may provide a novel approach to treat DMD and other muscle diseases that arise due to defects in the dystrophin glycoprotein complex. A video that contrasts kyphosis, gait, joint contractures, and mobility in *mdx/utr*$^{-/-}$ and *α7BX2-mdx/utr*$^{-/-}$ mice can be accessed at http://www.jcb.org/cgi/content/full/152/6/1207.

Key words: α7β1 integrin • muscular dystrophy • dystrophin • utrophin • neuromuscular junction

Introduction

The defective association of skeletal and cardiac muscle with their surrounding basal lamina underlies the pathologies associated with a variety of muscular dystrophies and cardiomyopathies (Matsumura and Campbell, 1994; Hayashi et al., 1998; Lim and Campbell, 1998). Duchenne muscular dystrophy (DMD)[1] is a congenital X-linked myopathy that is caused by a lack of the dystrophin protein and affects approximately 1 in 3,300 males. Patients with DMD experience progressive muscle deterioration and debilitation that severely restricts mobility. Death due to cardiac and respiratory failure usually occurs in the second decade of life.

Mutations in the dystrophin gene result in a lack of dystrophin, a 427-kD protein localized at the cytoplasmic side of the plasma membrane of skeletal and cardiac muscle cells (Monaco et al., 1986; Matsumura and Campbell, 1994; Campbell, 1995). In association with dystroglycans, syntrophins, and sarcoglycans, dystrophin links the cell cytoskeleton to laminin in the extracellular matrix. In the absence of one or more components of the dystrophin linkage system, the association of fibers with the surrounding basal lamina is compromised, leading to the myopathy observed. Thus, the molecular continuity between the extracellular matrix and the cell cytoskeleton is essential for the structural and functional integrity of muscle.

The integrins are αβ heterodimeric receptors that bind extracellular matrix proteins and interact with the cell cytoskeleton (Hynes, 1992). The α7β1 integrin is a laminin receptor on skeletal and cardiac muscle (von der Mark et al., 1991; Song et al., 1992) and serves as a transmembrane link between the basal lamina and muscle fibers. Multiple isoforms of the α7 and β1 chains are generated by developmentally regulated RNA splicing, resulting in a family of receptors

✪The online version of this article contains supplemental material.

Address correspondence to Stephen J. Kaufman, Department of Cell and Structural Biology, University of Illinois, B107 Chemical and Life Sciences Laboratory, Urbana, IL 61801. Tel.: (217) 333-3521. Fax: (217) 244-1648. E-mail: stephenk@uiuc.edu

[1]*Abbreviations used in this paper:* AChR, acetylcholine receptor; DMD, Duchenne muscular dystrophy; fMyHC, fetal myosin heavy chain; MCK, muscle creatine kinase, MRI, magnetic resonance imaging; NMJ, neuromuscular junction.

with diverse structures and functions (for reviews see Hodges and Kaufman, 1996; Burkin and Kaufman, 1999).

The α7 integrin chain is encoded by a single autosomal gene on human chromosome 12q13 (Wang et al., 1995). Three alternative cytoplasmic domains (α7A, α7B, and α7C) and two extracellular domain variants (X1 and X2) of the protein have been identified (Collo et al., 1993; Song et al., 1993; Ziober et al., 1993). Four additional alternatively spliced isoforms of the extracellular domain have been predicted by nucleotide sequence analysis (Leung et al., 1998; Vignier et al., 1999).

The β1 chain cytoplasmic domain also undergoes developmentally regulated alternative splicing. β1A is the most common isoform of the β1 chain and is expressed in a wide variety of tissues including replicating myoblasts. The alternative β1D form is generated upon differentiation of myoblasts to myofibers (van der Flier et al., 1995; Zhidkova et al., 1995; Belkin et al., 1996, 1997).

Mutations in the genes that encode the many components of the dystrophin glycoprotein complex cause a variety of muscular dystrophies. Mutations in the α7 gene also cause congenital myopathies (Hayashi et al., 1998). Thus, both the integrin- and dystrophin-mediated transmembrane linkage systems contribute to the functional integrity of skeletal muscle. Interestingly, there is an increase in the amount of α7 transcript and protein in DMD patients and *mdx* mice (the mouse model that has a mutation in its dystrophin gene) (Hodges et al., 1997). This led us to suggest that enhanced expression of the integrin may partially compensate for the absence of the dystrophin glycoprotein complex (Hodges et al., 1997; Burkin and Kaufman, 1999).

Utrophin, a protein homologous to dystrophin, is also increased in DMD patients and *mdx* mice (Law et al., 1994; Pons et al., 1994). Utrophin associates with many of the same proteins as dystrophin and further increasing utrophin may, in part, also compensate for the absence of dystrophin (Tinsley et al., 1996).

Although DMD patients (Monaco et al., 1986) and *mdx* mice (Bulfield et al., 1984; Sicinski et al., 1989) both lack dystrophin, the pathology that develops in the *mdx* mouse is much less severe than that observed in humans. The differences in the extent of pathology may be due to several factors, including the enhanced expression and altered localization of utrophin (Law et al., 1994; Pons et al., 1994) and the α7 integrin chain (Hodges et al., 1997) in *mdx* mice. In addition, differences in utilization of skeletal muscles by humans compared with mice in captivity may also contribute to the decreased level of pathology seen in *mdx* mice. In contrast, *mdx/utr*$^{-/-}$ mice lack both dystrophin and utrophin and have a phenotype that is similar to that seen in DMD patients. These double mutant mice develop severe progressive muscular dystrophy and die prematurely between 4 and 20 wk of age (Deconinck et al., 1997b; Grady et al., 1997b).

To explore the hypothesis that enhanced expression of the α7β1 integrin may compensate for the absence of the dystrophin glycoprotein complex and reduce the development of severe muscle disease, transgenic mice were made that express the rat α7 chain. We report that *mdx/utr*$^{-/-}$ mice with enhanced expression of the α7BX2 chain isoform show greatly improved longevity and mobility compared with nontransgenic *mdx/utr*$^{-/-}$ mice. Transgenic mice maintained weight and had reduced spinal curvature (kyphosis) and joint contractures. Transgenic expression of the α7BX2 chain also reduced the degree of mononuclear cell infiltration and expression of fetal myosin heavy chain (fMyHC) in muscle fibers. Together these results show that enhanced expression of α7BX2β1D integrin significantly reduces the development of muscular dystrophy.

Materials and Methods

Muscle Creatine Kinase-α7BX2 Integrin Construct

The cDNA encoding the rat α7BX2 integrin isoform was cloned into pBK-RSV vector (Stratagene) downstream of the 3.3-kb mouse muscle creatine kinase (MCK) promoter and the mouse α7 integrin cell surface localization signal sequence using the restriction sites AatII and KpnI. The MCK promoter was provided by Dr. Stephen Hauschka (University of Washington, Seattle, WA). The construct was verified by DNA sequencing. Previous studies have shown that the MCK promoter is only active in heart and skeletal muscle (Jaynes et al., 1986; Johnson et al., 1989; Shield et al., 1996). The expression and functionality of the MCK-α7BX2 integrin construct were verified by transfecting C2C12 myoblasts (Burkin et al., 1998, 2000).

Production of Transgenic mdx/utr$^{-/-}$ Mice

The MCK-α7BX2 construct was gel purified. *mdx/utr*$^{+/-}$ female mice were superovulated, mated to *mdx/utr*$^{+/-}$ male mice, and fertilized oocytes were collected. The MCK-α7BX2 construct was microinjected into male pronuclei, and injected oocytes were placed into pseudopregnant mice at the University of Illinois Transgenic Animal Facility. Resulting pups were weaned at 3 wk of age, and genomic DNA was isolated from 0.5-cm tail clips using a DNA isolation kit (Promega). Primers (MCK1, 5′-caagctgcacgcctgggtcc-3′; and AATII, 5′-ggcacccatgacgtccagattgaag-3′), used to amplify between the MCK promoter and the α7 integrin cDNA, produced a 455-bp fragment only in transgenic mice. Transgenic *mdx/utr*$^{+/-}$ male mice were bred with *mdx/utr*$^{+/-}$ female mice to produce transgenic *α7BX2-mdx/utr*$^{-/-}$ offspring. The *mdx/utr*$^{+/-}$ mice (Grady et al., 1997b) used in these experiments were provided by Dr. Joshua Sanes (Washington University, St. Louis, MO).

The *mdx* mutation was screened by the amplification-resistant mutation system described by Amalfitano and Chamberlain (1996). A new forward primer (Int22-306F, 5′-catagttattaatgcatagatattcag-3′) upstream of the *mdx* mutation site was used to yield a larger, 275-bp band. The status of the utrophin gene was analyzed by PCR using the primers 553, 554, and 22803 described previously by Grady et al. (1997a). C57BL6 × SJ6 mice were used as wild-type controls.

Antibodies and Reagents

For immunofluorescence analysis, the mouse monoclonal antibody O26 was used to detect the transgenic rat α7 chain. Polyclonal anti-α7CDA (345) and anti-α7CDB (347) were used in Western blots to detect the α7A and α7B cytoplasmic domains, respectively (Song et al., 1993; Martin et al., 1996). The amino acid sequences of the mouse and rat α7 chain cytoplasmic domains are identical, thus these antisera will detect both species with equal affinity. Peptides used to make these polyclonal antibodies were used as blocking controls. Rabbit polyclonal antibodies to the cytoplasmic domains of the β1A and β1D integrin chains were provided by Dr. W.K. Song (K-JIST, Kwang-ju, Korea; Kim et al., 1999). Dystrophin was detected using an antidystrophin monoclonal antibody (MANDRA1) (Sigma-Aldrich). Antiutrophin monoclonal antibody (NCL-DRP2) was purchased from Novacastra. The anti-fMyHC monoclonal antibody 47A was a gift from Dr. Peter Merrifield (University of Western Ontario, London, Ontario, Canada). The anti-creatine kinase monoclonal antibody was obtained from ADI Diagnostics. Acetylcholine receptor (AChR) clusters were detected with rhodamine-labeled α-bungarotoxin (Molecular Probes). FITC-labeled donkey anti–mouse and anti–rabbit antibodies were purchased from Jackson ImmunoResearch Laboratories.

Western Blot Analysis

Samples of muscle tissue were extracted in 200 mM octyl-β-D-glucopyranoside or 1% NP-40 in 50 mM Tris-HCl, pH 7.4, 2 mM PMSF, 1:200 dilution of Protease Cocktail Set III (Calbiochem), 1 mM $CaCl_2$, and 1 mM

$MgCl_2$ at 4°C for 1 h. The supernatants were collected and protein concentrations were determined using Bradford assays. Equal amounts of extracted muscle proteins were separated on 8% polyacrylamide-SDS gels at 40 mA for 50 min, and the protein was transferred to nitrocellulose filters. Blocked filters were incubated with 1:500 dilutions of either polyclonal anti-α7CDA (345), anti-α7CDB (347), or anti-β1D antibody. HRP-linked anti–rabbit secondary antibody (Jackson ImmunoResearch Laboratories) was used to detect primary antibodies. Immunoreactive protein bands were detected using an ECL kit (Amersham Pharmacia Biotech). Specificity of the bands was determined using the blocking peptides used to raise the antibodies. Blots were reprobed with an anti-creatine kinase antibody. The intensities of the α7 bands were compared with creatine kinase and to total protein stained with Ponceau S using ImageQuant software. Comparable results were obtained by both methods.

Southern Blot Analysis

Mouse genomic DNA was isolated from whole blood or liver using a genomic DNA isolation kit (Promega). DNA was cleaved with EcoRI and KpnI at 3 U/μg of DNA for 16 h. DNA fragments were separated on 0.8% agarose gels and alkaline transferred to Hybond-XL nylon membranes (Amersham Pharmacia Biotech) (Sambrook et al., 1989). A 367-bp probe from the rat α7 3′-untranslated domain was isolated. The probe was directly labeled with HRP using a North2South nonradioactive kit (Pierce Chemical Co.). The hybridized blots were washed following the manufacturer's instructions. Probes were detected using an ECL substrate. Blots were exposed to x-ray film for 1–30 min.

Immunofluorescence

Quadriceps muscles from 10-wk-old wild-type male *mdx, mdx/utr*$^{-/-}$, and *α7BX2-mdx/utr*$^{-/-}$ mice were embedded in OCT compound (Tissue-Tek) and frozen in liquid nitrogen–cooled isopentane. Using a Leica CM1900 series cryostat, 10-μm sections were cut and placed on microscope slides coated with 1% gelatin, 0.05% chromium potassium sulfate. Sections were fixed in −20°C acetone for 1 min, rehydrated in 1× PBS for 10 min, and blocked in PBS containing 10% horse serum for 15 min. The rat α7 chain was detected using 5 μg/ml of purified O26 monoclonal antibody directly labeled with Alexa 488 (Molecular Probes). The anti-β1D antibody was used at a 1:100 dilution in 1% horse serum in PBS. The antidystrophin antibody was used at a 1:100 dilution, whereas antiutrophin and anti-fMyHC antibodies were diluted 1:2 in 1% horse serum in PBS. Rhodamine-labeled α-bungarotoxin was used at a 1:3,000 dilution to detect neuromuscular junctions (NMJs).

Endogeneous mouse immunoglobulin was blocked before the addition of monoclonal antibodies using 60 μg/ml goat anti–mouse monovalent Fabs (Jackson ImmunoResearch Laboratories) in 1% horse serum in PBS for 30 min at room temperature. Slides were then washed three times for 5 min in 1% horse serum in PBS. Primary antibodies were added for 1 h at room temperature. Slides were washed three times for 5 min in 1% horse serum in PBS. Primary antibodies were detected with a 1:100 dilution of FITC-labeled donkey anti–mouse or anti–rabbit antibody in 1% horse serum in PBS. Slides were mounted using Vectorshield mountant (Vector Laboratories). Localization of the antibody was observed with a ZEISS Photomicroscope III. Images were acquired with a Sony DXC9000 color video CCD camera using SiteCam software and a ZEISS Axiocam digital camera (see Fig. 10).

Histology

10-μm cryosections from the quadriceps muscles of 5-, 8-, and 10-wk-old wild-type, *mdx, mdx/utr*$^{-/-}$, and transgenic *mdx/utr*$^{-/-}$ mice were placed on uncoated slides and stained with hematoxylin and eosin. The occurrence of central nuclei was scored in ≥1,000 fibers in two mice from each line. The extent of mononuclear cell infiltration was estimated as the percentage of fields (40× objective) in which two or more clusters (>10 cells) of mononuclear cells were detected. At least 80 fields in four sections from each of the duplicate mice were scored.

Electron Microscopy

Sternomastoid muscles from 5-wk-old animals were fixed in 2% glutaraldehyde and 2.5% paraformaldehyde in 0.2 M Sorenson's phosphate buffer, embedded in LX-112 epoxy (Ladd Research Industries), sectioned at 0.1 μm using a Reichert Ultracut E Ultramicrotome, stained with uranyl acetate and lead citrate, and viewed with a Hitachi H-600 transmission electron microscope at a 20,000× magnification.

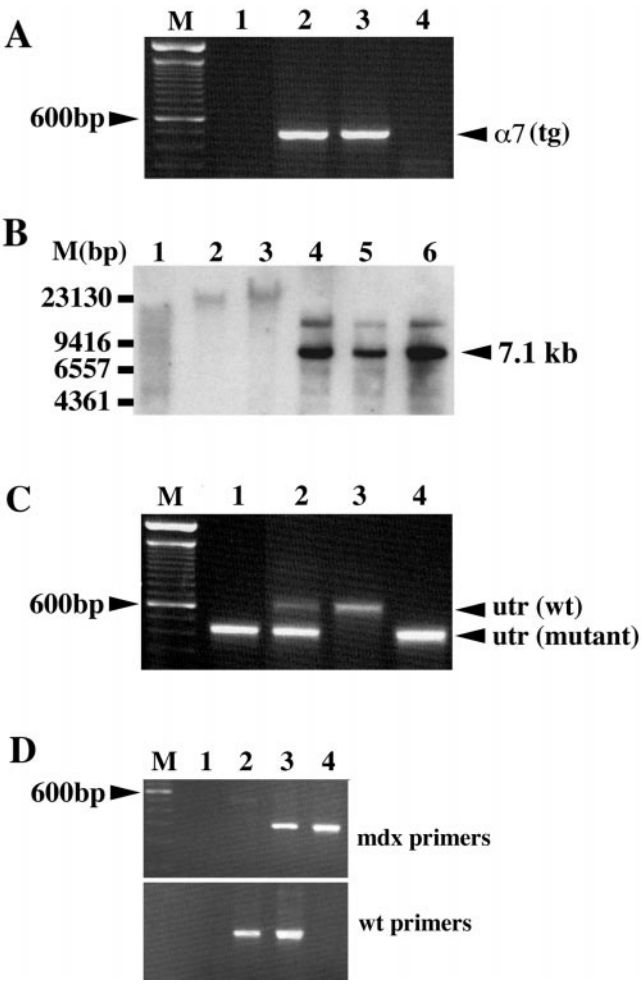

Figure 1. Genotyping transgenic *α7BX2-mdx/utr*$^{-/-}$ mice. (A) The α7BX2 transgene (tg) was detected by PCR using primers that amplify between the MCK promoter and the α7 cDNA sequence. Lanes 2 and 3 are positive for the MCK-α7BX2 transgene. (B) Southern blot analysis using a rat α7-specific probe of EcoRI- and KpnI-digested genomic DNA. The 7.1-kb band corresponding to the rat transgene construct is detected in lanes 4–6. A higher 14.2-kb transgene dimer was also detected. Samples in these lanes are from *α7BX2-mdx/utr*$^{-/-}$ mice. DNA in lanes 1–3 are from nontransgenic mice. (C) Determining the status of the utrophin gene by PCR. Only mutant *utr* alleles are detected in lanes 1 and 4, identifying *utr*$^{-/-}$ mice. One wild-type (wt) and one mutant allele are amplified in lane 2, identifying a *utr*$^{+/-}$ mouse. Lane 3 is wild-type at both *utr* loci. (D) Determining the status of the dystrophin gene by PCR. The *mdx* primer set detects the point mutation in the dystrophin gene, whereas the wt primers detect only the wild-type allele. Mouse 2 is wild-type at the dystrophin locus, mouse 3 is heterozygous (*mdx*/+), and mouse 4 is *mdx*. Lane 1 contains no DNA.

X-Ray and Magnetic Resonance Imaging

Spinal curvature (kyphosis) in 10-wk-old *mdx*, *mdx/utr*, and transgenic *α7BX2-mdx/utr*$^{-/-}$ mice was visualized by x-ray imaging using a Siemens Heliodent 70 x-ray machine (model D3104). X-rays were taken at 70 kVp and 7 mA. At least two mice of each genotype were analyzed.

Magnetic resonance imaging (MRI) of 10-wk-old wild-type, *mdx*, *mdx/utr*$^{-/-}$, and *α7BX2-mdx/utr*$^{-/-}$ mice was used to visualize soft tissues. Mice were imaged at 1-mm thickness using a 4.7 T/31 cm Surrey Medical Imaging Spectrophotometer. At least two mice of each genotype were analyzed.

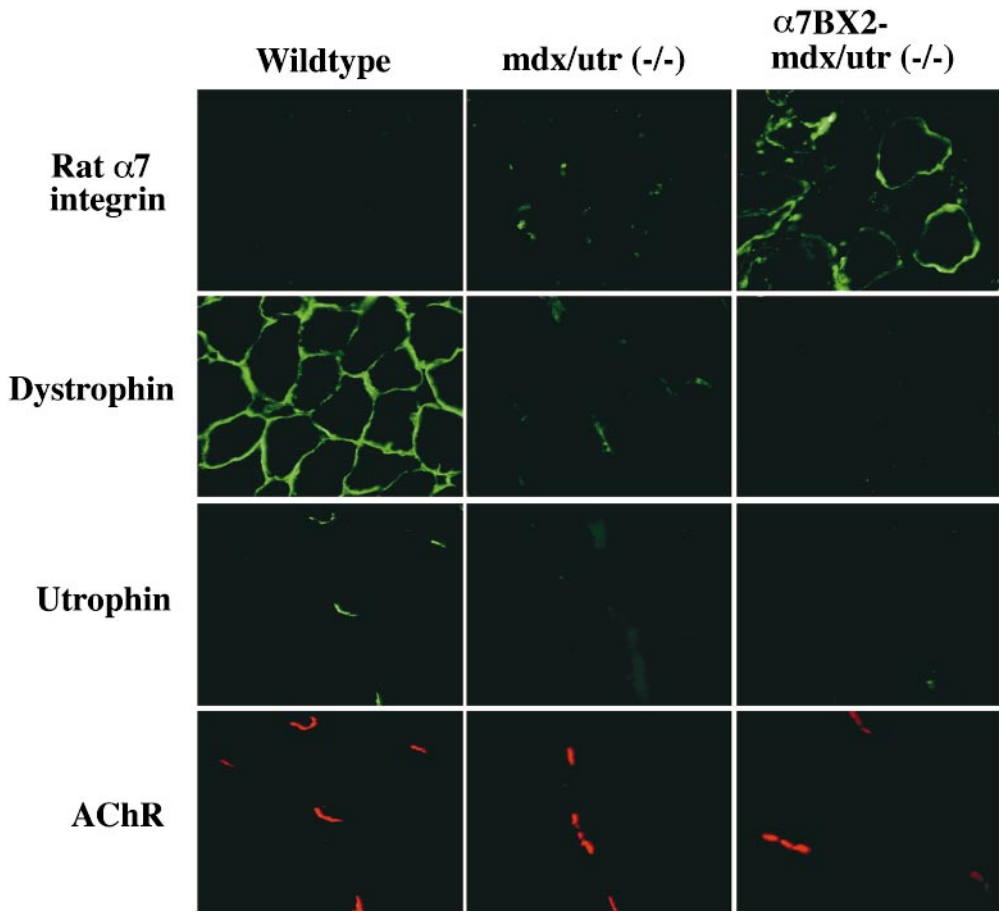

Figure 2. Expression of the rat α7 protein in mouse muscle. Immunofluorescence analysis of hindlimb cryosections using monoclonal antibodies against the rat α7 integrin chain, dystrophin, and utrophin. AChRs were stained with rhodamine-labeled α-bungarotoxin to identify NMJs, the sites of normal utrophin localization. The rat α7 protein is only detected in transgenic mice and localizes to the membrane of muscle fibers. The lack of dystrophin and utrophin in both transgenic and nontransgenic *mdx/utr*$^{-/-}$ mice confirms their genotypes. The fluorescent specks seen in the *mdx/utr*$^{-/-}$ muscle stained with mouse antidystrophin, antiutrophin, and anti-α7 integrin antibodies are also evident in the absence of primary antibody and are due to residual staining with secondary anti–mouse antibody.

Statistical Analysis

Survival data from 84 *mdx/utr*$^{-/-}$ mice and 43 transgenic *α7BX2-mdx/utr*$^{-/-}$ mice were analyzed using the Kaplan-Meier method (Kaplan and Meier, 1958). Survival curves were generated for both populations and the data were compared using log-rank (Peto et al., 1977) and Wilcoxon (Conover, 1980) statistical tests.

Online Supplemental Material

A video that contrasts kyphosis, gait, joint contractures, and mobility in *mdx/utr*$^{-/-}$ and *α7BX2-mdx/utr*$^{-/-}$ mice can be viewed at http://www.jcb.org/cgi/content/full/152/6/1207.

Results

Production of Transgenic Mice Expressing the Rat α7BX2 Chain

To test the hypothesis that the α7β1 integrin linkage system can alleviate severe muscle disease, transgenic mice were produced that express the rat α7 chain. DNA encoding the rat α7 integrin α7BX2 isoform, under the transcriptional control of the mouse MCK promoter, was cloned and shown to have biological activity in vitro (Burkin et al., 1998). The 3.3-kb MCK promoter limits transcription to differentiated skeletal and cardiac muscle, confining the effects of overexpression to these tissues (Donoviel et al., 1996). The 7.1-kb construct, MCK-α7BX2, was used to express the rat integrin in *mdx/utr*$^{-/-}$ mice. Due to the mortality of the double knockout mice, the rat transgene was initially introduced into a heterozygous (*mdx/utr*$^{+/-}$) background, and these animals were then bred to produce double knockout transgenic offspring. The ratio of offspring followed expected Mendelian genetics, indicating that the transgenic expression of the rat α7 integrin did not have an obvious effect on embryonic development. Two independent lines of transgenic mice were produced: α7BX2#2 and α7BX2#9. In this report, the data from the α7BX2#2 line are presented, but similar results were obtained with both.

The presence of the rat α7 transgene was detected by both PCR and Southern blot analyses. Using MCKI and AATII primers, a 455-bp product was amplified only in transgenic mice (Fig. 1 A). Southern blot analysis produced a strong 7.1-kb band only in transgenic mice. This is the expected size of the EcoRI and KpnI digested MCK-α7BX2 construct (Fig. 1 B). A weak 14.2-kb band was also detected by Southern blot analysis, suggesting that a portion of the constructs had lost one of these restriction sites.

The status of the utrophin gene was analyzed by PCR using the primers 553, 554, and 22803 described previously (Grady et al., 1997a). The 640-bp product is amplified when the wild-type utrophin allele is present, whereas the 450-bp product is amplified when the utrophin mutant allele is present (Fig. 1 C).

The status of the dystrophin gene was determined by the amplification-resistant mutation detection system (Amalfitano and Chamberlain, 1996). Using the *mdx*-specific primer set, a 275-bp mutant allele is detected, whereas in separate reactions the wild-type–specific primer set de-

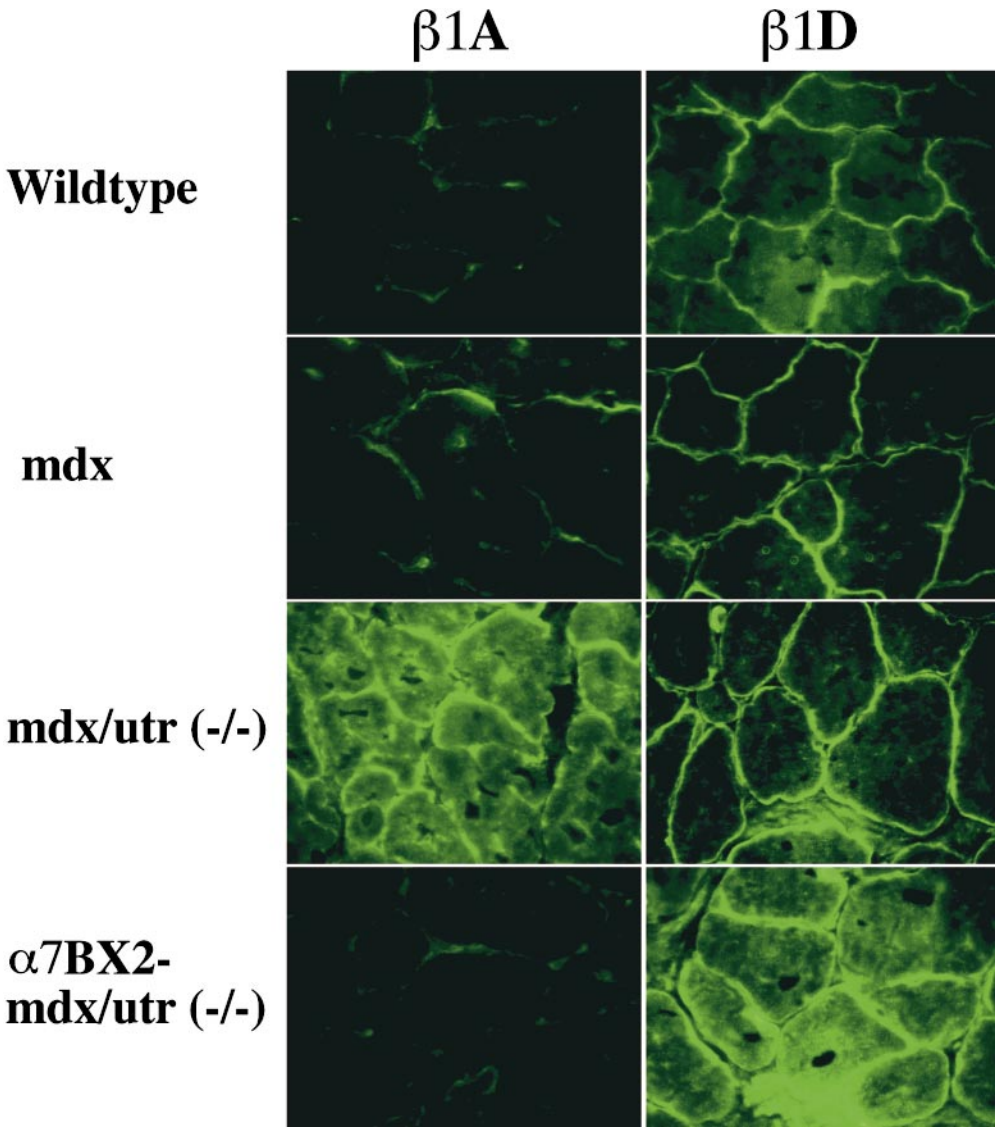

Figure 3. Immunofluorescence of β1 integrin isoforms in the hindlimb of 8-wk-old wild-type, *mdx*, *mdx/utr*$^{-/-}$, and *α7BX2-mdx/utr*$^{-/-}$ mice. β1A integrin is elevated in muscle fibers of *mdx/utr*$^{-/-}$ mice compared with wild-type and *mdx* animals. In contrast, β1A levels are normal in *α7BX2-mdx/utr*$^{-/-}$ mice. Compared with wild-type, an increase in β1D is detected in both *mdx* and *mdx/utr*$^{-/-}$ muscle. *α7BX2-mdx/utr*$^{-/-}$ mice show an additional increase in β1D compared with both *mdx* and *mdx/utr*$^{-/-}$ mice.

tects a 275-bp wild-type allele. Fig. 1 D shows three different genotypes at the dystrophin locus. Mouse 2 is wild-type at the dystrophin locus, mouse 3 is heterozygous (*mdx/+*), and mouse 4 is *mdx*.

Protein expression from the rat α7 chain transgene was determined by immunofluorescence analysis of cryosections using the rat-specific α7 monoclonal antibody O26 (Fig. 2). The rat α7 chain was only detected by immunofluorescence in the muscle of transgenic mice (Fig. 2). Immunofluorescence also showed the absence of dystrophin in muscle fibers and the absence of utrophin at NMJs in both transgenic and nontransgenic *mdx/utr*$^{-/-}$ mice (Fig. 2). The fluorescent specks seen in Fig. 2 upon staining *mdx/utr*$^{-/-}$ muscle with mouse antidystrophin, antiutrophin, and anti-α7 integrin antibodies are visible in the absence of primary antibody and are due to residual staining with secondary anti–mouse antibody.

The alternative spliced form of the β1 integrin chain, β1D, is expressed in differentiated skeletal and cardiac muscle (van der Flier et al., 1995; Zhidkova et al., 1995; Belkin et al., 1996). Compared with the β1A, β1D may form stronger linkages between the cell cytoskeleton and extracellular matrix (Belkin et al., 1997). Immunofluorescence analysis showed β1A levels were elevated in fibers of *mdx/utr*$^{-/-}$ mice compared with wild-type and *mdx* animals. This is indicative of muscle that is not fully differentiated. In contrast, *α7BX2-mdx/utr*$^{-/-}$ mice had normal levels of β1A integrin. Immunofluorescence and Western blot analysis showed that *mdx* and *mdx/utr*$^{-/-}$ mice have more cell surface β1D chain than wild-type mice. This increase in β1D coincided with an increase in endogenous α7 chain in nontransgenic *mdx* and *mdx/utr*$^{-/-}$ mice as well as total α7 in *α7BX2-mdx/utr*$^{-/-}$ mice. The *α7BX2-mdx/utr*$^{-/-}$ mice also had an additional 1.5-fold more β1D compared with *mdx/utr*$^{-/-}$ mice (Fig. 3 and Fig. 4 C). Thus, an increase in the α7BX2β1D integrin is promoted by increased expression of the α7 transgene.

As reported previously, *mdx* mice express approximately twofold more α7 integrin mRNA than wild-type controls (Hodges et al., 1997). No further increase in α7 protein was detected in the *mdx/utr*$^{-/-}$ animals. The amount of α7BX2 protein in the *α7BX2-mdx/utr*$^{-/-}$ mouse hindlimb detected by Western blots was 2.0–2.3-fold greater than the endogenous α7BX2 chain in *mdx/utr*$^{-/-}$

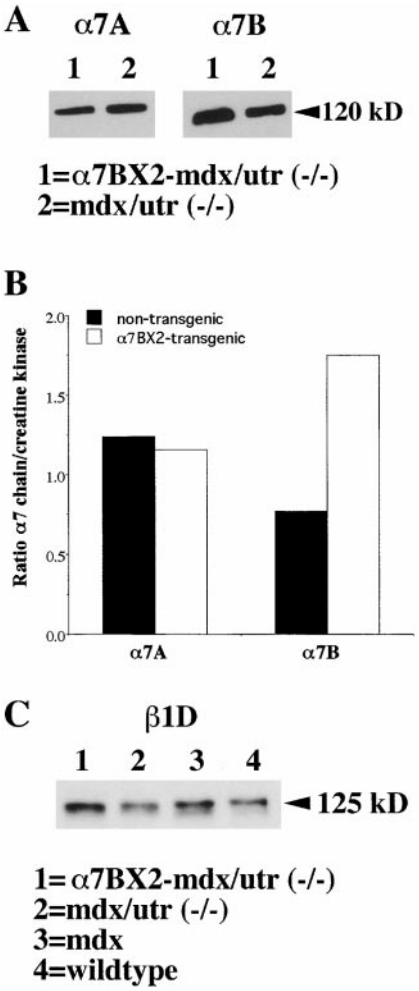

Figure 4. Transgenic expression of α7BX2 increases the amount of β1D in hindlimb muscle. (A) Western blot showing more α7B is detected in transgenic mice compared with nontransgenic mice, whereas α7A is constant. (B) The blots were reprobed with anti-creatine kinase antibody. The creatine kinase levels were used to normalize the amounts of α7A and α7B proteins in each sample. The levels of α7A/creatinine kinase in both transgenic and nontransgenic mice remained constant. In contrast, the α7B/creatinine kinase ratio is 2.3-fold higher in the α7BX2 transgenic mice compared with the nontransgenic animal. Comparisons relative to total protein stained with Ponceau S indicate a 2.0-fold increase. (C) β1D integrin from 8 wk hindlimb muscle. Less β1D is detected in *mdx/utr*$^{-/-}$ mice compared with *α7BX2-mdx/utr*$^{-/-}$ mice. Compared with total protein, an increase of approximately 1.5-fold more β1D was detected in the transgenic versus nontransgenic mice. Similar results were obtained in duplicate experiments.

mice (Fig. 4, A and B). As expected, the levels of α7AX2 were equivalent in the transgenic and nontransgenic mice (Fig. 4, A and B).

α7BX2-mdx/utr$^{-/-}$ *Mice Exhibit Increased Longevity and Mobility*

Longevity was significantly extended in the α*7BX2-mdx/utr*$^{-/-}$ transgenic mice (Fig. 5). Kaplan-Meier survival analysis (Kaplan and Meier, 1958) of 84 nontransgenic and 43 transgenic *mdx/utr*$^{-/-}$ mice demonstrated that the observed differences in survival of these populations were statistically significant ($P < 0.001$). Log-rank (Peto et al., 1977) and

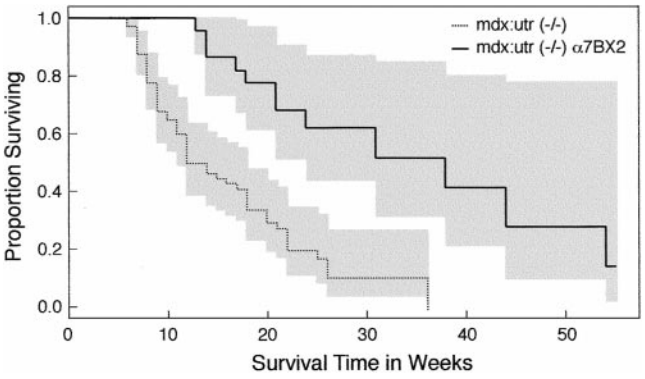

Figure 5. Kaplan-Meier survival curves of 43 *α7BX2-mdx/utr*$^{-/-}$ and 84 *mdx/utr*$^{-/-}$ mice. Wilcoxon and log-rank tests show that the *α7BX2-mdx/utr*$^{-/-}$ and *mdx/utr*$^{-/-}$ mice populations have distinct survival curves ($P < 0.001$). The *α7BX2-mdx/utr*$^{-/-}$ mice survive threefold longer than nontransgenic *mdx/utr*$^{-/-}$ mice with a median life expectancy of 38 wk. In contrast, nontransgenic *mdx/utr*$^{-/-}$ mice have a median life expectancy of 12 wk (95% confidence intervals are indicated by shading).

Wilcoxon rank-sum tests (Conover, 1980) showed that the difference in survival emerged soon after birth and was maintained throughout the observed lifetime of the animals. The *mdx/utr*$^{-/-}$ mice used in these experiments developed severe muscular dystrophy and 50% died before 12 wk of age. The median age at death of the transgenic *mdx/utr*$^{-/-}$ mice was 38 wk, a threefold increase over that observed in nontransgenic *mdx/utr*$^{-/-}$ littermates. These findings were consistent in both male and female mice. The oldest *α7BX2-mdx/utr*$^{-/-}$ mouse was killed at 64 wk of age.

Compared with *mdx* mice that exhibit minimal pathology, *mdx/utr*$^{-/-}$ mice do not maintain weight. Instead, these mice undergo a crisis period that results in weight loss and premature death at 4–20 wk of age (Deconinck et al., 1997b; Grady et al., 1997b). In contrast, *α7BX2-mdx/utr*$^{-/-}$ transgenic mice did not show sudden weight loss. Animal weight stabilized between 20 and 25 g (Fig. 6). No signifi-

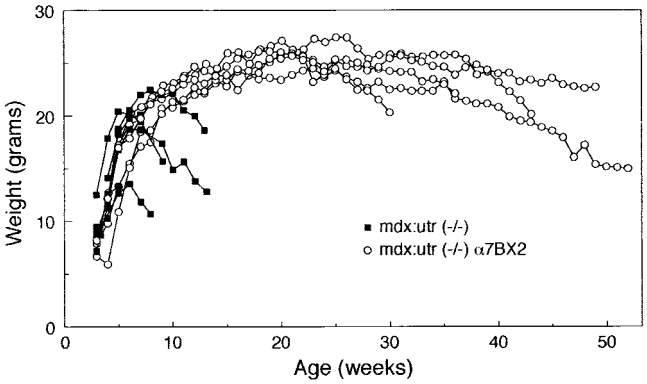

Figure 6. Weight gain versus survival in five representative *mdx/utr*$^{-/-}$ mice and α*7BX2-mdx/utr*$^{-/-}$ mice. The majority of nontransgenic *mdx/utr*$^{-/-}$ mice undergo a crisis at 5–10 wk of age that results in a sudden loss of weight and premature death. Most transgenic *mdx/utr*$^{-/-}$ mice live longer and maintain weight. Eventually these too will go through a crisis that results in weight loss. The mean life span of the *mdx/utr*$^{-/-}$ mice illustrated here is 10.4 wk; the mean life span of the *α7BX2-mdx/utr*$^{-/-}$ mice illustrated here is 41.8 wk.

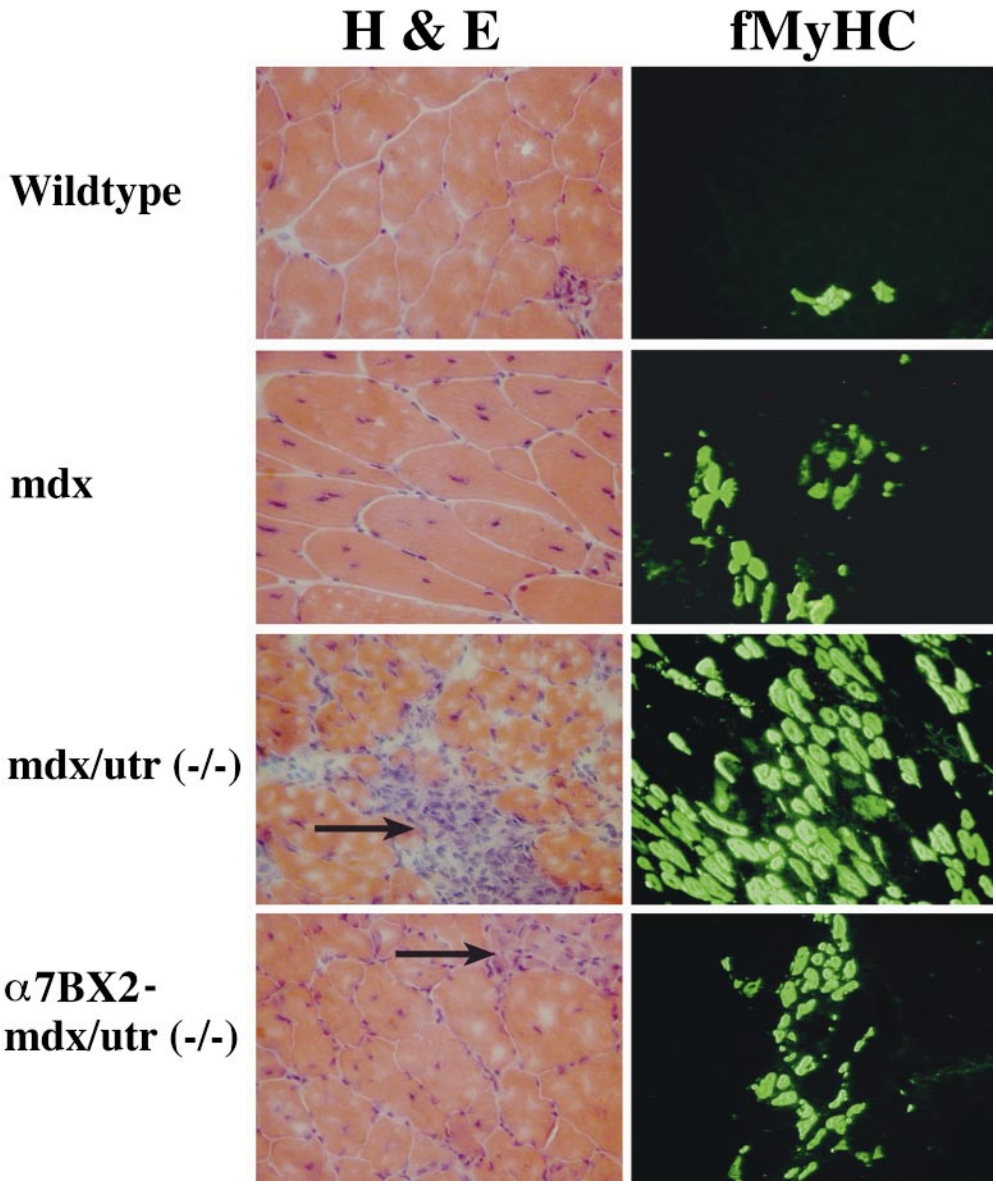

Figure 7. Histology of hindlimbs from 10-wk-old wild-type, *mdx*, *mdx/utr*$^{-/-}$, and *α7BX2-mdx/utr*$^{-/-}$ mice. Hematoxylin and eosin (H & E) staining reveals abundant central nuclei in *mdx*, *mdx/utr*$^{-/-}$, and *α7BX2-mdx/utr*$^{-/-}$ mice. Mononuclear cell infiltration (arrows) and expression of fMyHC are extensive in the *mdx/utr*$^{-/-}$ mice, but are reduced in the *α7BX2-mdx/utr*$^{-/-}$ transgenic animals, indicating less degeneration and more stable regeneration in these mice.

cant differences were found in the weights of *mdx* mice compared with *α7BX2-mdx* mice 3–30 wk of age. Thus, extra *α7BX2* chain itself does not promote weight gain.

By 8 wk of age, *mdx/utr*$^{-/-}$ mice exhibited limited mobility and a waddling gait. In contrast, *α7BX2-mdx/utr*$^{-/-}$ littermates had highly improved mobility compared with *mdx* mice. A video that contrasts kyphosis, gait, joint contractures, and mobility in *mdx/utr*$^{-/-}$ and *α7BX2-mdx/utr*$^{-/-}$ transgenic mice is accessible at http://www.jcb.org/cgi/content/full/152/6/1207.

Enhanced Expression of the α7BX2 Chain Stabilizes Regeneration in mdx/utr$^{-/-}$ *Mice*

Nuclei are normally localized along the periphery of myofibers, whereas in regenerating muscle nuclei are centrally located (DiMario et al., 1991). Regeneration is also accompanied by a transient reversion to expression of fetal isoforms of myosin heavy chain (fMyHC) (Matsuda et al., 1983; Saad et al., 1987). Hindlimb sections from 5-, 8-, and 10-wk-old wild-type, *mdx*, *mdx/utr*$^{-/-}$, and *α7BX2-mdx/utr*$^{-/-}$ mice were stained with hematoxylin and eosin to determine the extent of mononuclear infiltration and centrally located nuclei (Fig. 7 and Table I). Immunofluorescence of fMyHC was also determined. Degeneration and regeneration that are characteristic of muscle disease occur earlier in *mdx/utr*$^{-/-}$ animals compared with *mdx* mice (Fig. 7 and Table I). These results are consistent with the earlier onset of necrosis and cell infiltration reported previously in these animals (Deconinck et al., 1997b; Grady et al., 1997b). The occurrence of central nuclei in *α7BX2-mdx/utr*$^{-/-}$ mice was similar to that in *mdx/utr*$^{-/-}$ mice, indicating that enhanced expression of

Table I. Percentage of Fibers with Central Nuclei

Mice	5 wk	8 wk	10 wk
Wild-type	2.6	1.3	2.7
mdx	33.0	65.6	70.9
mdx/utr$^{-/-}$	79.0	78.4	75.3
α7BX2-mdx/utr$^{-/-}$	62.1	71.7	63.9

Sections of hindlimb muscle from 5-, 8-, and 10-wk-old mice were stained with hematoxylin and eosin. Nuclear localization was scored in ≥1,000 fibers in each animal.

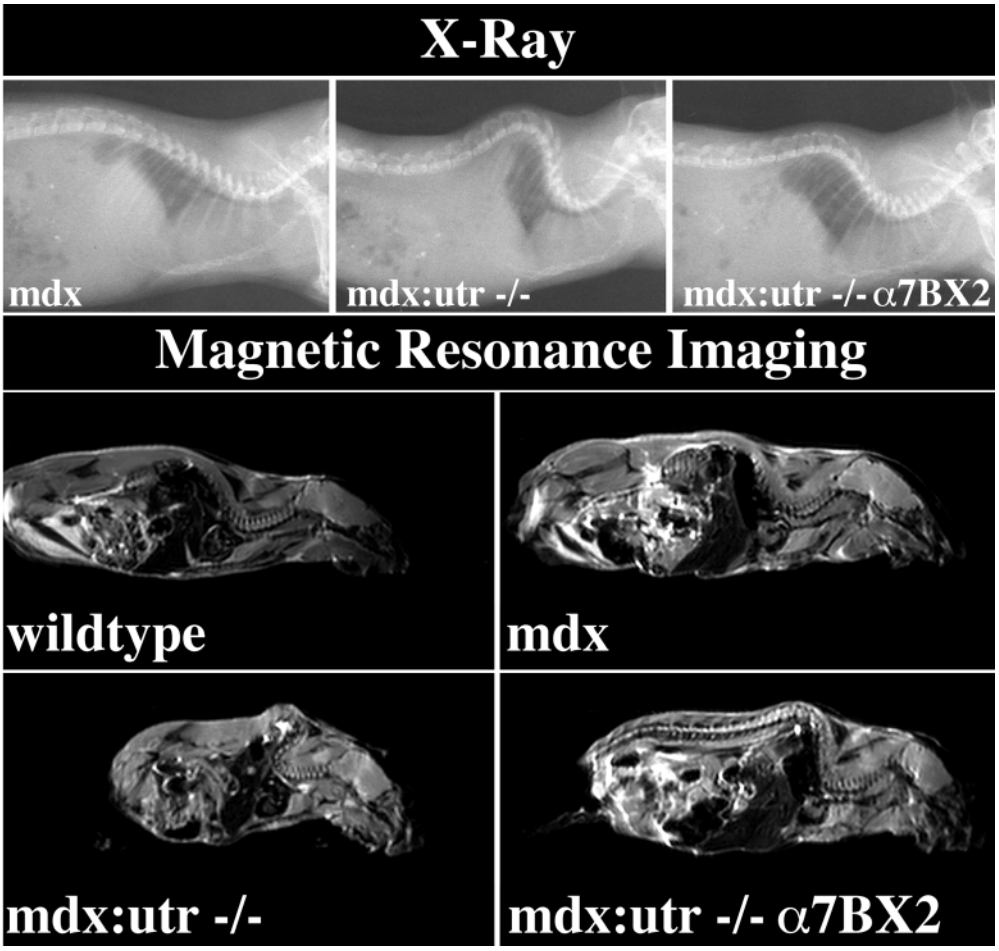

Figure 8. X-ray and MRI of normal and dystrophic mice. Top three panels, the severe spinal curvature (kyphosis) and constriction of the rib cage in *mdx/utr*$^{-/-}$ mice are largely reduced in the α7BX2 transgenic animals; bottom four panels, MRI of midsagittal sections reveals that kyphosis and reduction of pulmonary volume in *mdx/utr*$^{-/-}$ mice are largely alleviated in transgenic mice.

the integrin does not prevent early degeneration and regeneration. Likewise, fMyHC expression was most extensive at 5 wk in the *mdx/utr*$^{-/-}$ and *α7BX2-mdx/utr*$^{-/-}$ mice. In contrast, *mdx* mice exhibited very little fMyHC at 5 wk. At 8 wk, fMyHC was elevated in *mdx* mice, and at 10 wk it was reduced, indicating that a cycle of degeneration and regeneration was followed by stabilization. The shift from the β1A to β1D chain supports this conclusion. At all ages examined, the extent of fMyHC expression in the *α7BX2-mdx/utr*$^{-/-}$ animals was intermediate between that found in the *mdx* and *mdx/utr*$^{-/-}$ animals. In the 8- and 10-wk-old transgenic *mdx/utr*$^{-/-}$ mice, fMyHC expression approached that in *mdx* mice (Fig. 7). This decreased expression of fMyHC in *α7BX2-mdx/utr*$^{-/-}$ mice paralleled the greater integrity of tissue seen in the 8- and 10-wk-old transgenic animals compared with the *mdx/utr* $^{(-/-)}$ mice. The extensive mononuclear cell infiltration observed in the *mdx/utr*$^{-/-}$ mice (89–97% positive fields) was also partially reduced in the *α7BX2-mdx/utr*$^{-/-}$ animals (Fig. 7). The percentage of fields with cell infiltration was reduced approximately 17 and 19% in 5- and 8-wk-old transgenic versus nontransgenic *mdx/utr*$^{-/-}$ mice, respectively. This represents a minimal estimate since the areas of cell infiltration were considerably larger in the nontransgenic animals (Fig. 7). Thus, enhanced expression of the α7β1 integrin does not alter the initial degenerative cycle, but once regeneration has taken place, the additional integrin appears to stabilize muscle integrity, reducing muscle pathology.

Kyphosis and Joint Contractures Are Alleviated in α7BX2-mdx/utr$^{-/-}$ *Mice*

Severe curvature of the spine (kyphosis) in DMD patients and *mdx/utr*$^{-/-}$ mice is due to a failure of the muscles that would normally support the spinal column (Oda et al., 1993). X-ray images showed that both kyphosis and rib cage compression were markedly reduced in *α7BX2-mdx/utr*$^{-/-}$ mice compared with *mdx/utr*$^{-/-}$ littermates (Fig. 8). This was confirmed by whole body MRI which visualized not only the tissues surrounding the spinal column, but bundles of muscle fibers, the heart, lung, and other soft tissues. The reduction in kyphosis promoted by the enhanced expression of integrin in the *α7BX2-mdx/utr*$^{-/-}$ animals is likely a major factor in their survival. Kyphosis results in the diaphragm being pushed forward, compromising lung capacity and diaphragm function, and thereby contributing to cardiopulmonary failure. A partial reduction of kyphosis may therefore have dramatic effects on survival.

A hallmark of diseased musculature is the failure to extend limb muscles, resulting in joint contractures. Hindlimb joint contractures are conspicuous in *mdx/utr*$^{-/-}$ mice but are markedly reduced in the *α7BX2-mdx/utr*$^{-/-}$ mice (Fig. 9). The reduction in hindlimb joint contractures allows the mice to have greatly improved mobility.

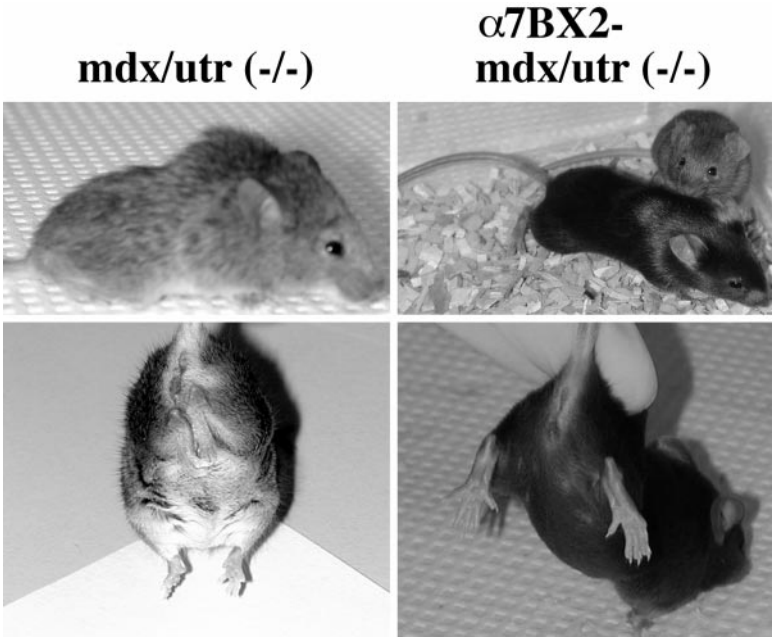

Figure 9. Severe spinal curvature (kyphosis) and hindlimb clasping (joint contractures) are largely reduced in mice expressing the rat α7BX2 transgene.

Structural Changes in the NMJs of α7BX2-mdx/utr$^{-/-}$ Mice

The NMJs in *utr*$^{-/-}$ mice exhibit a significant reduction in the number of synaptic folds and density of AChRs (Deconinck et al., 1997a; Grady et al., 1997a). This is exacerbated in *mdx/utr*$^{-/-}$ mice which show even greater reduction in postsynaptic folding and AChR density (Deconinck et al., 1997b; Grady et al., 1997b). The postsynaptic plate of the NMJ in the *mdx/utr*$^{-/-}$ mice appears en face as discrete boutons rather than as a continuous folded structure (Grady et al., 1997b; Rafael et al., 2000).

Since the α7β1 integrin is normally found at NMJs (Martin et al., 1996) and participates in the clustering of AChRs in C2C12 cells (Burkin et al., 1998, 2000), we compared the structure of NMJs from 5-wk-old wild-type, *mdx/utr*$^{-/-}$, and *α7BX2-mdx/utr*$^{-/-}$ mice (Fig. 10). Longitudinal sections of hindlimb muscles were stained with rhodamine-labeled α-bungarotoxin, and images of en face sections of the postsynaptic membrane were analyzed. Fluorescence staining of the NMJs of *mdx/utr*$^{-/-}$ mice appeared less intense compared with wild-type mice and showed discrete boutons. In contrast, most NMJs from *α7BX2-mdx/utr*$^{-/-}$ mice appeared more continuous. The postsynaptic membrane in longitudinal sections prepared from sternomastoid muscles was examined by EM. The normal folded morphology of the postsynaptic membrane is markedly reduced in the *mdx/utr*$^{-/-}$ animals, as reported previously (Deconinck et al., 1997b; Grady et al., 1997b). As seen in Fig. 10, postsynaptic folding was partially restored in the *α7BX2-mdx/utr*$^{-/-}$ mice. Thus, enhanced levels of the α7β1 integrin help maintain the normal structure of the NMJ.

Discussion

Our results demonstrate for the first time that enhanced expression of the α7β1 integrin can alleviate the development of muscular dystrophy and significantly extend longevity. Mice lacking both dystrophin and utrophin were used in this study because in the absence of both proteins direct substitution of dystrophin with utrophin is precluded. This results in the development of severe muscular dystrophy and premature death, symptoms that closely resemble those seen in DMD (Deconinck et al., 1997b; Grady et al., 1997b).

The *α7BX2-mdx/utr*$^{-/-}$ mice reported here have ~2.0–2.3-fold more α7BX2 chain than their nontransgenic littermates. The β1D chain, partner to α7, is also increased in the α7BX2 transgenic mice. The increased levels of α7β1 integrin led to a threefold extension in median survival time, markedly improved mobility, and reduced kyphosis and joint contractures in the transgenic *mdx/utr*$^{-/-}$ mice. Kaplan-Meier survival analysis of the transgenic and nontransgenic *mdx/utr*$^{-/-}$ mice shows that the extension of longevity due to expression of the transgene is statistically significant and is evident early and throughout the life of the animals.

The survival times of the *mdx/utr*$^{-/-}$ mice in these experiments differ slightly from those reported previously. The original reported longevity of the *mdx/utr*$^{-/-}$ mice bred from the *mdx/utr*$^{+/-}$ line used to produce the animals in our experiments was 4–14 wk (Grady et al., 1997b). More recently, a life span of 4–20 wk has been reported (Grady et al., 1999) and occasional longer living mice have been noted (Sanes, J.R., personal communication). We too have noted some "outliers": 6 of 84 *mdx/utr*$^{-/-}$ mice survived beyond 22 wk, with the oldest mouse dying at 36 wk of age. The transgenic and nontransgenic mice with extended life spans were reevaluated for expression of dystrophin and utrophin by PCR and immunofluorescence and were again found deficient in both. Nevertheless, *α7BX2-mdx/utr*$^{-/-}$ mice are clearly distinct in longevity, mobility, and histology from nontransgenic littermates. The median life span of the α7BX2-*mdx/utr*$^{-/-}$ mice was 38 wk, whereas the median life span for those not receiving the transgene was 12 wk.

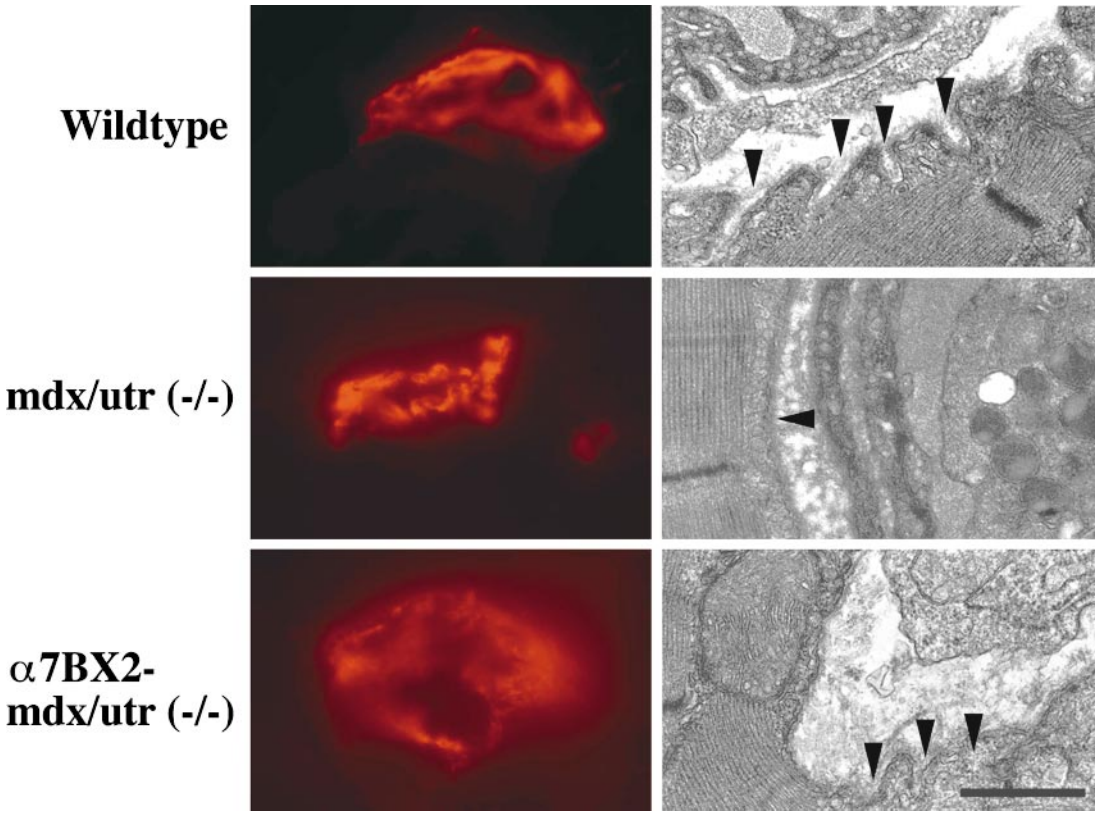

Figure 10. Structure of the NMJ in 5-wk-old wild-type, *mdx/utr*$^{-/-}$, and *α7BX2-mdx/utr*$^{-/-}$ mice. (Left) En face views of AChRs in the postsynaptic membrane detected with rhodamine-labeled α-bungarotoxin. In wild-type mice, the junctions appear continuous, folded, and uninterrupted. In *mdx/utr*$^{-/-}$ mice, the distribution of AChRs is discontinuous and organized into discrete boutons. The organization of the postsynaptic membrane in *α7BX2-mdx/utr*$^{-/-}$ transgenic mice has a more continuous (normal) pattern. (Right) Ultrastructural changes in the NMJ. The postsynatic membrane of wild-type mice is highly folded (arrowheads). In contrast, *mdx/utr*$^{-/-}$ mice have little or no membrane folding. Expression of the α7BX2 transgene in *mdx/utr*$^{-/-}$ mice results in a postsynaptic membrane with partially restored folding (arrowheads). Bar, 1 μm.

Although the mechanism by which enhanced expression of the α7β1 integrin alleviates the development of the dystrophic phenotype is not currently understood, multiple effects that result from additional α and β integrin chains are possible.

Expression of the β1D chain is restricted to differentiated skeletal and cardiac muscle (van der Flier et al., 1995; Zhidkova et al., 1995; Belkin et al., 1996, 1997). In contrast, the β1A chain is present in a wide variety of cell types including myogenic precursor cells. The β1D cytoplasmic domain may act to arrest the progression of myoblast proliferation and alter subcellular localization and affinity of α7β1 for its ligand and the association of the α7β1 with the cell cytoskeleton (Belkin et al., 1997). Therefore, increased β1D expression in α7BX2 transgenic mice may increase the interaction between the extracellular matrix, sarcolemma, and the cell cytoskeleton, stabilizing muscle integrity. Moreover, β1A, characteristic of nonmuscle cells and undifferentiated muscle, is increased in *mdx/utr*$^{-/-}$ and decreased in the transgenic *mdx/utr*$^{-/-}$ animals. The shift from β1A and increased β1D reflects fewer mononuclear cell infiltrates and increased stability of muscle fibers in the rescued mice.

The α7BX2 integrin chain is normally concentrated at neuromuscular and myotendinous junctions (Martin et al., 1996) and at intrafascicular junctions (Duxson, M., personal communication). In patients with DMD and in *mdx* and *mdx/utr*$^{-/-}$ mice, endogenous expression of the α7 integrin protein is increased, and the α7BX2 isoform is also found extrajunctionally (Hodges et al., 1997). This increase in expression and redistribution of α7β1 integrin in dystrophic mice is also seen with utrophin that is normally confined to NMJs (Matsumura et al., 1992). Immunolocalization of integrin encoded by the rat α7 transgene detected with anti–rat α7 antibodies shows that the rat α7 protein is also distributed more globally in the *α7BX2-mdx/utr*$^{-/-}$ animals. Enhanced expression of the integrin therefore contributes to the mechanical integration and stability between muscle fibers and at their junctional sites. Other possible mechanisms may also underlie how the α7β1 integrin rescues *mdx/utr*$^{-/-}$ mice.

Whereas the MCK promoter drives transcription in skeletal and cardiac muscle (Donoviel et al., 1996), enhanced expression of the α7β1 integrin in the heart may also contribute to the rescue of these animals. However, expression of utrophin in skeletal muscle, but not cardiac muscle, of *mdx/utr*$^{-/-}$ mice increased survival and reduced pathology (Rafael et al., 1998). These observations suggest that the loss of skeletal muscle integrity is the major factor in the development muscle pathology in *mdx/utr*$^{-/-}$ mice.

The role of the α7β1 integrin in the formation of the postsynaptic membrane (Burkin et al., 1998, 2000) suggests

that increased integrin expression may enhance the development and stability of the NMJs. Dystrophin and utrophin are also concentrated at the postsynaptic membrane and *mdx*, *utr*$^{-/-}$, and *mdx/utr*$^{-/-}$ mice show progressive alterations of the ultrastructure of these sites (Deconinck et al., 1997b; Grady et al., 1997b). Whereas wild-type and *utr*$^{-/-}$ mice have NMJ endplates that are highly folded and continuous, *mdx* and *mdx/utr*$^{-/-}$ mice show discontinuous NMJs that are described as discrete "boutons" (Grady et al., 1997a,b; Rafael et al., 2000). Whereas both *mdx* and *utr*$^{-/-}$ mice show a reduction in the number of synaptic folds compared with wild-type mice, *mdx/utr*$^{-/-}$ mice show even fewer synaptic folds (Deconinck et al., 1997b; Grady et al., 1997b). Transgenic expression of the α7BX2 chain appears to maintain the normal structure of the postsynaptic membrane in *mdx/utr*$^{-/-}$ mice.

In the absence of dystrophin, there is an increase in total muscle calcium (Bertorini et al., 1982) and an elevation of intracellular calcium ($[Ca^{2+}]_i$) in isolated dystrophic myofibers (Turner et al., 1988). These increases have been attributed to leaky calcium channels in dystrophic muscle compared with normal muscle. The $[Ca^{2+}]_i$ increase may activate Ca^{2+}-dependent proteolysis and increase muscle degeneration (Denetclaw et al., 1994). $[Ca^{2+}]_i$ levels are also regulated by signaling through the α7β1 integrin (Kwon et al., 2000), suggesting that this integrin may contribute to the maintenance of calcium levels in myofibers. If so, the transgenic expression of the α7BX2 chain may regulate the activity of calcium channels, stabilizing $[Ca^{2+}]_i$ levels in *mdx/utr*$^{-/-}$ myofibers and reducing Ca^{2+}-dependent proteolysis and muscle degeneration.

Enhanced expression of the α7 integrin may contribute to additional changes in the expression of other proteins, both within the cell and in the extracellular matrix. For example, matrix stability or modeling may potentiate both mechanical and signal transduction capacities of muscle (Colognato et al., 1999). This dual role for the integrin is consistent with analyses of *α7*$^{-/-}$ mice. The myotendinous junctions of fast fibers are compromised in α7-deficient mice (Mayer et al., 1997). These myofibers also exhibit a partial shift from β1D to β1A integrin and activation of the c-Raf-1/mitogen-activated protein kinase 2 signaling pathway. These changes cause a reduction of integrin-dependent association of fibers and the basal lamina, contributing to the dystrophy that develops in these mice (Saher and Hildt, 1999). As shown here, increased α7 chain leads to increased β1D.

A broad phenotype is seen in children with congenital muscular dystrophies that arise from mutations in the α7 gene (Hayashi et al., 1998). These patients exhibit congenital myopathy, delayed motor milestones, and severe impairment of mobility. These phenotypes are consistent with a role for α7β1 integrin in the formation and stability of the postsynaptic membrane, myotendinous junctions, and overall stability of muscle integrity.

Since enhanced expression of the α7β1 integrin can alleviate many of the symptoms of severe muscular dystrophy in *mdx/utr*$^{-/-}$ mice, it appears that the integrin- and dystrophin-mediated linkage systems between myofibers and the extracellular matrix are in many ways functionally complementary mechanisms. As such, the enhanced expression of the α7β1 integrin may be a novel approach to alleviate DMD and treat α7 integrin congenital muscular dystrophies. Moreover, increasing integrin levels may prove effective in reducing the development of other muscular dystrophies and cardiomyopathies that arise from compromised expression of other components of the dystrophin glycoprotein complex.

This paper is dedicated to the memory of Dr. Kiichi Arahata, a distinguished scientist who taught us much about muscle and its diseases.

We gratefully acknowledge the generous gift of the *mdx/utr*$^{+/-}$ mice provided by Dr. Joshua Sanes (Washington University) and the MCK promoter and advice kindly provided by Drs. Stephen Hauschka and Jean Buskin (University of Washington). We thank Dr. Jonathan Henry (University of Illinois) for his helpful discussions of the X-ray and MRI analyses and Mr. Eric Chaney for his skillful assistance with the EM. Mice were generated at the University of Illinois Transgenic Animal Facility under the direction of Dr. Matt Wheeler, with the expert technical assistance of Ms. Melissa Hentges. MRI data were obtained at the University of Illinois Medical Resonance Imaging Center under the direction of Dr. Paul Lauterbur, with the technical assistance of Ms. Sherrie Frydenger.

Supported by the Muscular Dystrophy Association and the National Institutes of Health.

Submitted: 30 October 2000
Revised: 17 January 2001
Accepted: 22 January 2001

References

Amalfitano, A., and J.S. Chamberlain. 1996. The *mdx*-amplification-resistant mutation system assay, a simple and rapid polymerase chain reaction-based detection of the mdx allele. *Muscle Nerve.* 19:1549–1553.

Belkin, A.M., N.I. Zhidkova, F. Balzac, F. Altruda, D. Tomatis, A. Maier, G. Tarone, V.E. Koteliansky, and K. Burridge. 1996. Beta 1D integrin displaces the beta 1A isoform in striated muscles: localization at junctional structures and signaling potential in nonmuscle cells. *J. Cell Biol.* 132:211–216.

Belkin, A.M., S.F. Retta, O.Y. Pletjushkina, F. Balzac, L. Silengo, R. Fassler, V.E. Koteliansky, K. Burridge, and G. Tarone. 1997. Muscle beta1D integrin reinforces the cytoskeleton–matrix link: modulation of integrin adhesive function by alternative splicing. *J. Cell Biol.* 139:1583–1595.

Bertorini, T.E., S.K. Bhattacharya, G.M. Palmieri, C.M. Chesney, D. Pifer, and B. Baker. 1982. Muscle calcium and magnesium content in Duchenne muscular dystrophy. *Neurology.* 32:1088–1092.

Bulfield, G., W.G. Siller, P.A. Wight, and K.J. Moore. 1984. X chromosome-linked muscular dystrophy (mdx) in the mouse. *Proc. Natl. Acad. Sci. USA.* 81:1189–1192.

Burkin, D.J., and S.J. Kaufman. 1999. The α7β1 integrin in muscle development and disease. *Cell Tissue Res.* 296:183–190.

Burkin, D.J., M. Gu, B.L. Hodges, J.T. Campanelli, and S.J. Kaufman. 1998. A functional role for specific spliced variants of the α7β1 integrin in acetylcholine receptor clustering. *J. Cell Biol.* 143: 1067–1075.

Burkin, D.J., J.E. Kim, M. Gu, and S.J. Kaufman. 2000. Laminin and α7β1 integrin regulate agrin-induced clustering of acetylcholine receptors. *J. Cell Sci.* 113:2877–2886.

Campbell, K.P. 1995. Three muscular dystrophies: loss of cytoskeleton-extracellular matrix linkage. *Cell.* 80:675–679.

Collo, G., L. Starr, and V. Quaranta. 1993. A new isoform of the laminin receptor integrin alpha 7 beta 1 is developmentally regulated in skeletal muscle. *J. Biol. Chem.* 268:19019–19024.

Colognato, H., D.A. Winkelmann, and P.D. Yurchenco. 1999. Laminin polymerization induces a receptor–cytoskeleton network. *J. Cell Biol.* 145:619–631.

Conover, W.J. 1980. Practical Nonparametric Statistics. 2nd ed. John Wiley & Sons, New York. 493 pp.

Deconinck, A.E., A.C. Potter, J.M. Tinsley, S.J. Wood, R. Vater, C. Young, L. Metzinger, A. Vincent, C.R. Slater, and K.E. Davies. 1997a. Postsynaptic abnormalities at the neuromuscular junctions of utrophin-deficient mice. *J. Cell Biol.* 136:883–894.

Deconinck, A.E., A.C. Potter, J.M. Tinsley, S.J. Wood, R. Vater, C. Young, L. Metzinger, A. Vincent, C.R. Slater, and K.E. Davies. 1997b. Utrophin-dystrophin deficient mice as a model for Duchenne muscular dystrophy. *Cell.* 90:717–727.

Denetclaw, W.F., Jr., F.W. Hopf, G.A. Cox, J.S. Chamberlain, and R.A. Steinhardt. 1994. Myotubes from transgenic mdx mice expressing full-length dystrophin show normal calcium regulation. *Mol. Biol. Cell.* 5:1159–1167.

DiMario, J.X., A. Uzman, and R.C. Strohman. 1991. Fiber regeneration is not persistent in dystrophic (mdx) mouse skeletal muscle. *Dev. Biol.* 148:314–321.

Donoviel, D.B., M.A. Shield, J.N. Buskin, H.S. Haugen, C.H. Clegg, and S.D. Hauschka. 1996. Analysis of muscle creatine kinase gene regulatory elements in skeletal and cardiac muscles of transgenic mice. *Mol. Cell. Biol.* 16:

1649–1658.
Grady, R.M., J.P. Merlie, and J.R. Sanes. 1997a. Subtle neuromuscular defects in utrophin-deficient mice. *J. Cell Biol*. 136:871–882.
Grady, R.M., H. Teng, M.C. Nichol, J.C. Cunningham, R.W. Wilkinson, and J.R. Sanes. 1997b. Skeletal and cardiac myopathies in mice lacking utrophin and dystrophin: a model for Duchenne muscular dystrophy. *Cell*. 90:729–738.
Grady, R.M., R.W. Grange, K.S. Lau, M.M. Maimone, M.C. Nichol, J.T. Stull, and J.R. Sanes. 1999. Role for alpha-dystrobrevin in the pathogenesis of dystrophin-dependent muscular dystrophies. *Nat. Cell Biol.* 1:215–220.
Hayashi, Y.K., E. Engvall, Arikawa-Hirasawa, K. Goto, R. Koga, I. Nonaka, H. Sugita, and K. Arahata. 1993. Abnormal localization of laminin subunits in muscular dystrophies. *J. Neurol. Sci*. 119:53–64.
Hayashi, Y.K., F.-L. Chou, E. Engvall, M. Ogawa, C. Matsuda, S. Hirabayashi, K. Yokochi, B.L. Ziober, R.H. Kramer, S.J. Kaufman, E. Ozawa, et al. 1998. Mutations in the integrin α7 gene cause congenital myopathy. *Nat. Genet*. 19:94–97.
Hodges, B.L., and S.J. Kaufman. 1996. Developmental regulation and functional significance of alternative splicing of NCAM and α7β1 integrin in skeletal muscle. *Basic Appl. Myol*. 6:437–446.
Hodges, B.L., Y.K. Hayashi, I. Nonaka, W. Wang, K. Arahata, and S.J. Kaufman. 1997. Altered expression of the α7β1 integrin in human and murine muscular dystrophies. *J. Cell Sci*. 110:2873–2881.
Hynes, R.O. 1992. Integrins: versatility, modulation, and signaling in cell adhesion. *Cell.* 69:11–25.
Jaynes, J.B., J.S. Chamberlain., J.N Buskin, J.E. Johnson, and S.D. Hauschka. 1986. Transcriptional regulation of the muscle creatine kinase gene and related expression in transfected mouse myoblasts. *Mol. Cell. Biol*. 6:2855–2864.
Johnson, J.E., B.J. Wold, and S.D. Hauschka. 1989. Muscle creatine kinase sequence elements regulating skeletal and cardiac muscle expression in transgenic mice. *Mol. Cell. Biol*. 9:3393–3399.
Kaplan, E.L., and P. Meier. 1958. Nonparametric estimation from incomplete observations. *J. Am. Stat. Assoc*. 53:457–481.
Kim, Y.Y., C.S. Lim, Y.H. Song, J.H. Ahn, D.E. Park, and W.K. Song. 1999. Cellular localization of α3β1 integrin isoforms in association with myofibrillogenesis during cardiac myocyte development in culture. *Cell Adhes. Commun.* 7:85–97.
Kwon, M.S., C.S. Park, K.-R. Choi, C.-S. Park, J. Ahnn, J.I. Kim, S.H. Eom, S.J. Kaufman, and W.K. Song. 2000. Calreticulin couples calcium release and calcium influx in α7β1 integrin-mediated calcium signaling. *Mol. Cell. Biol.* 11:1433–1443.
Law, D.J., D.L. Allen, and J.G. Tidball. 1994. Talin, vinculin and DRP (utrophin) concentrations are increased at the *mdx* myotendinous junctions following onset of necrosis. *J. Cell Sci*. 107:1477–1483.
Leung, E., S.P. Lim, R. Berg, Y. Yang, J. Ni, S. Wang, and G.W. Krissansen. 1998. A novel extracellular domain variant of the human integrin α7 subunit generated by alternative intron splicing. *Biochem. Biophys. Res. Commun*. 243:317–325.
Lim, L.E., and K.P. Campbell. 1998. The sarcoglycan complex in limb-girdle muscular dystrophy. *Curr. Opin. Neurol.* 11:443–452.
Martin, P.T., S.J. Kaufman, R.H. Kramer, and J.R. Sanes. 1996. Synaptic integrins: selective association of the α1 and α7A, and α7B subunits with the neuromuscular junction. *Dev. Biol*. 174:125–139.
Matsuda, R., D. Spector, and R.C. Strohman. 1983. Regenerating adult chicken skeletal muscle and satellite cell cultures express embryonic patterns of myosin and tropomyosin isoforms. *Dev. Biol.* 100:478–488.
Matsumura, K., and K.P. Campbell. 1994. Dystrophin-glycoprotein complex: its role in the molecular pathogenesis of muscular dystrophies. *Muscle Nerve*. 17:2–15.
Matsumura, K., J.M. Ervasti, K. Ohlendieck, S.D. Kahl, and K.P. Campbell. 1992. Association of dystrophin-related protein with dystrophin-associated proteins in mdx mouse muscle. *Nature.* 360:588–591.
Mayer, U., G. Saher, R. Fassler, A. Bornemann, F. Echtermeyer, H. von der Mark, N. Miosge, E. Poschl, and K. von der Mark. 1997. Absence of integrin alpha 7 causes a novel form of muscular dystrophy. *Nat. Genet*. 17:318–323.
Monaco, A.P., R.L. Neve, C. Colletti-Feener, C.J. Bertelson, D.M. Kurnit, and L.M. Kunkel. 1986. Isolation of candidate cDNAs for portions of the Duchenne muscular dystrophy gene. *Nature.* 323:646–650.
Oda, T., N. Shimizu, K. Yonenobu, K. Ono, T. Nabeshima, and S. Kyoh. 1993. Longitudinal study of spinal deformity in Duchenne muscular dystrophy. *J. Pediatr. Orthop.* 13:478–488.
Peto, R., M.C. Pike, P. Armitage, N.E. Breslow, D.R. Cox, S.V. Howard, N. Mantel, K. McPherson, J. Peto, and P.G. Smith. 1977. Design and analysis of randomized clinical trials requiring prolonged observation of each patient. II. Analysis and examples. *Brit. J. Cancer*. 35:1–39.
Pons, F., A. Robert, J.F. Marini, and J.J. Leger. 1994. Does utrophin expression in muscles of mdx mice during postnatal development functionally compensate for dystrophin deficiency. *J. Neurol. Sci*. 122:162–170.
Rafael, J.A., J.M. Tinsley, A.C. Potter, A.E. Deconinck, and K.E. Davies. 1998. Skeletal muscle-specific expression of a utrophin transgene rescues utrophin-dystrophin deficient mice. *Nat. Genet*. 19:79–82.
Rafael, J.A., E.R. Townsend, S.E. Squire, A.C. Potter, J.S. Chamberlain, and K.E. Davies. 2000. Dystrophin and utrophin influence fiber type composition and post-synaptic membrane structure. *Hum. Mol. Genet.* 9:1357–1367.
Saad, A.D., T. Obinata, and D.A. Fischman. 1987. Immunochemical analysis of protein isoforms in thick myofilaments of regenerating skeletal muscle. *Dev. Biol.* 119:336–349.
Saher, G., and E. Hildt. 1999. Activation of c-Raf-1 kinase signal transduction pathway in alpha(7) integrin-deficient mice. *J. Biol. Chem.* 274:27651–27657.
Sambrook, J., E.F. Fritsch, and T. Maniatis. 1989. Molecular Cloning: A Laboratory Manual. 2nd ed., Vol. 2. Cold Spring Harbor Laboratory, Cold Spring Harbor, NY. 9.45–9.46.
Shield, M.A., H.S. Haugen, C.H. Clegg, and S.D. Hauschka. 1996. E-box sites and a proximal regulatory region of the muscle creatine kinase gene differentially regulate expression in diverse skeletal muscles and cardiac muscle of transgenic mice. *Mol. Cell. Biol*. 16:5058–5068.
Sicinski, P., Y. Geng, A.S. Ryder-Cook, E.A. Barnard, M.G. Darlison, and P.J. Barnard. 1989. The molecular basis of muscular dystrophy in the mdx mouse: a point mutation. *Science.* 244:1578–1580.
Song, W.K., W. Wang, R.F. Foster, D.A. Bielser, and S.J. Kaufman. 1992. H36-α7 is a novel integrin alpha chain that is developmentally regulated during skeletal myogenesis. *J. Cell Biol.* 117:643–667.
Song, W.K., W. Wang, H. Sato, D.A. Bielser, and S.J. Kaufman. 1993. Expression of α7 integrin cytoplasmic domains during skeletal muscle development: alternate forms, conformational change, and homologies with serine/threonine kinases and tyrosine phosphatases. *J. Cell Sci.* 106:1139–1152.
Tinsley, J.M., A.C. Potter, S.R. Phelps, R. Fisher, J.I. Trickett, and K.E. Davies. 1996. Amelioration of the dystrophic phenotype of *mdx* mice using a truncated utrophin transgene. *Nature.* 384: 349–353.
Turner, P.R., T. Westwood, C.M. Regen, and R.A. Steinhardt. 1988. Increased protein degradation results from elevated free calcium levels found in muscle from *mdx* mice. *Nature.* 335:735–738.
van der Flier, A., I. Kuikman, C. Baudoin, R. van der Neut, and A. Sonnenberg. 1995. A novel beta 1 integrin isoform produced by alternative splicing: unique expression in cardiac and skeletal muscle. *FEBS Lett*. 369:340–344.
Vignier, N., B. Moghadaszadehm, F. Gary, J. Beckmann, U. Mayer, and P. Guicheney. 1999. Structure, genetic localization, and identification of the cardiac and skeletal muscle transcripts of the human integrin alpha 7 gene (ITGA). *Biochem. Biophys. Res. Commun*. 260:357–364.
von der Mark, H.J., J. Durr, A. Sonnenberg, K. von der Mark, R. Deutzmann, and S.I. Goodman. 1991. Skeletal myoblasts utilize a novel α1-series integrin and not α6β1 for binding to the E8 and T8 fragments of laminin. *J. Biol. Chem.* 266:23593–23601.
Wang, W., W. Wu, T. Desai, D.C. Ward, and S.J. Kaufman. 1995. Localization of the α7 integrin gene (ITGA7) on human chromosome 12q13: Clustering of integrin and *hox* genes implies parallel evolution of these gene families. *Genomics.* 26:563–570.
Zhidkova, N.I., A.M. Belkin, and R. Mayne. 1995. Novel isoform of beta 1 integrin expressed in skeletal and cardiac muscle. *Biochem. Biophys. Res. Commun*. 214:279–285.
Ziober, B.L., M.P. Vu, N. Waleh, J. Crawford, C.S. Lin, and R.H. Kramer. 1993. Alternative extracellular and cytoplasmic domains of the integrin α7 subunit are differentially expressed during development. *J. Biol. Chem.* 268: 26773–26783.